Pressure-induced enhancement of the critical current density in superconducting $YBa_2Cu_3O_x$ bicrystalline rings

T. Tomita and J. S. Schilling
Department of Physics, Washington University, CB 1105, One Brookings Drive, St. Louis, Missouri 63130, USA

L. Chen, B. W. Veal, and H. Claus
Materials Science Division, Argonne National Laboratory, 9700 South Cass Avenue, Argonne, Illinois 60439, USA

(Received 3 April 2006; published 31 August 2006; corrected 5 September 2006)

The dependence of the critical current density $J_c(T)$ on hydrostatic He-gas pressure to 0.6 GPa is determined for nearly optimally doped and strongly underdoped melt-textured $YBa_2Cu_3O_x$ bicrystalline rings containing single [001]-tilt grain boundaries (GBs) with mismatch angles θ from 0° to 31°. For all samples with $\theta > 0°$, J_c is found to increase rapidly under pressure, the rate of increase lying predominantly in the range +20 to +50 % GPa^{-1}. Within a simple tunneling model, this rate of increase is far too large to be accounted for by a decrease in the GB width W alone. Large oxygen relaxation phenomena in the GB are observed for all rings with finite θ, particularly if they are underdoped. A diagnostic method is introduced (pressure-induced J_c relaxation) which reveals a significant concentration of vacant oxygen sites in the GB region. A concerted effort to fill such sites with oxygen anions, as well as to chemically compress the GB itself, should lead to significant enhancements in J_c under ambient conditions.

DOI: 10.1103/PhysRevB.74.064517 PACS number(s): 74.62.Fj, 74.25.Sv, 74.72.Bk, 74.81.Bd

I. INTRODUCTION

Superconducting technologies have the potential to have a major impact on everyday life. The realization of this potential with the high-T_c cuprate oxides, however, has been hampered by two main shortcomings. (1) Superconducting transition temperatures remain at subambient levels, the highest known value at ambient pressure remaining pinned at $T_c \simeq 134$ K (Ref. 1) for more than a decade. (2) Grain boundaries (GBs) in polycrystalline materials are unable to tolerate large critical current densities $J_c \simeq 10^6 - 10^7$ A/cm^2, even at liquid He temperatures, particularly in high magnetic fields.[2,3] This "GB problem" can be avoided by utilizing epitaxially grown thin films; however, many applications are only feasible with bulk polycrystalline materials.

One way to strongly enhance the value of J_c in polycrystals is to utilize suitable texturing (grain alignment) procedures to reduce the mismatch angle between adjacent grains to less than 4°.[4,5] Another method is to properly prepare the GB region through Ca doping[6,7] or other means.[3] Very recent detailed TEM and EELS studies have attributed the success of Ca doping both to strong Ca segregation near the dislocation cores[8] and to the reduction in strains in the GB which reduces the depletion of oxygen anions in the GB region, thus enhancing the (hole) carrier concentration.[9] In either case oxygen depletion in the GB is a very important factor and leads to a serious reduction in J_c.

The oxygen concentration in the GB region, which likely differs significantly from that in the bulk, is thus a parameter of vital importance in the optimization of J_c, even as the oxygen content within a grain plays a major role in determining the value of T_c itself in the bulk superconductor.[10] Unfortunately, the determination of the oxygen concentration in the GB is quite difficult.[9] The concentration of charge carriers in the GB region changes not only with the oxygen concentration, but, in all likelihood, also with the manner in which the oxygen sites in the GB are occupied, in analogy with the well known oxygen ordering effects in the bulk of the high-T_c oxide cuprates.[11–16] These bulk effects have their origin in the appreciable mobility of oxygen anions in certain regions of the oxygen sublattice, even at temperatures somewhat below ambient.

$YBa_2Cu_3O_x$ (YBCO) is by far the most studied and most thoroughly characterized high-T_c superconductor; this is due to the fact that it was the first superconductor discovered with a transition temperature above that of liquid nitrogen[17] and because it has a great potential for applications.[18] In YBCO oxygen anions in the CuO chains possess significant mobility at ambient temperature, in contrast to oxygen anions in the CuO_2 planes.[11,13] The degree of local order assumed by the mobile oxygen anions changes as a function of both temperature and pressure: raising the temperature above ambient reduces the order in an equilibrated system, applying pressure at ambient temperatures enhances the order. The existence of pressure-induced oxygen ordering effects can thus be readily demonstrated by applying pressure at ambient temperature to enhance the local order, but releasing it at temperatures sufficiently low (<200 K for YBCO) that the oxygen anions are unable to diffuse back, thus effectively freezing in the higher degree of order.[12–16]

The degree of local oxygen ordering influences indirectly the charge carrier concentration n in the CuO_2 planes by changing the average valence of the ambivalent cations (in YBCO these are the Cu cations in the CuO chains,[11] in $Tl_2Ba_2CuO_{6+\delta}$ the Tl cations in the Tl_2O_2 double layer[12]). Since T_c is a sensitive function of n,[19] the degree of oxygen ordering may have a sizeable or even dominant effect on T_c.[12–16] In overdoped $Tl_2Ba_2CuO_{6+\delta}$, for example, the hydrostatic pressure dependence even changes sign from $dT_c/dP \simeq -8.9$ to +0.35 K/GPa depending on whether, respectively, oxygen-ordering effects occur or not.[12] Significant oxygen ordering effects in dT_c/dP have also been observed in $YBa_2Cu_3O_x$,[13,14] particularly for underdoped samples with

TABLE I. Values of properties and parameters obtained for $YBa_2Cu_3O_x$ bicrystalline rings in present study. See text for definitions of parameters. Lower-case letters identifying rings are also used in text and figure captions. $d\ln J_c/dP$ and $(d\ln J_c/dP)_{\text{intr}}$ are normally measured at 9 K. (An asterisk) indicates measured at 50 K. (The pound sign) indicates measured at 75 K.

ring	x	θ	OD×ID×h mm^3	T_c K	$\left(\frac{dT_c}{dP}\right)_{\text{RT/LT}}$ K GPa^{-1}	D/A A G^{-1} cm^{-2}	J_c(0 K) A cm^{-2}	β	$\left(\frac{d\ln J_c}{dP}\right)$ GPa^{-1}	$\left(\frac{d\ln J_c}{dP}\right)_{\text{intr}}$ GPa^{-1}	η
a	6.9	4°	4.93×3.45×1.89	91.8		23.8	119,000				
a′	6.9	4°	3.96×3.39×0.91	91.8	0.14/0.14	112	112,000	1.48(9)	0.28(4)#	0.25(2)#	0.12(4)#
b	6.9	18°	4.90×3.51×1.01	91.2		47.4	1,990	0.87(2)	0.30(2)*	0.24(2)*	0.19(4)*
b′	6.9	18°	4.99×3.54×1.06	91.8		44.0	480		0.06(2)		
b″	6.5	18°	4.95×3.45×1.21	60.8	4.2/3.2	36.9	269	0.70(2)	0.27(4)		
c	6.9	21°	4.97×3.38×1.79	92.1		23.4	790	0.87(2)	0.32(4)		
d	6.9	25°	3.90×2.06×0.57	91.8	−0.23/−0.09	45.1	1,450	0.87(2)	0.20(2)	0.16(2)	0.20(2)
e	6.9	30°	4.98×3.43×0.60	91.8	0.22/0.12	72.0	1,570	0.85(2)	0.26(2)	0.14(2)	>0.13(2)
g	6.9	31°	4.92×3.28×1.43	91.6		27.8	520		0.20(2)		
g′	6.9	31°	4.91×3.40×1.33	91.5		32.8	1,050		0.19(2)		
g″	6.5	31°	4.98×3.42×1.08	60.7	4.2/3.4	39.6	99	0.6(1)			
i	6.4	15°	4.98×3.50×0.92	49.8	5.9	51.9	43.1	0.77(2)	0.45(2)		
k	6.4	20°	4.98×3.54×0.94	51.8	5.3/2.7	49.9	134	0.74(2)	0.59(2)	0.21(2)	0.65(2)
m	6.9	0°	5.01×3.23×0.12	91.5	0.36/0.11	306	275,000		0.00(2)		
m′	6.86	0°	4.85×3.37×0.49	86.3	1.5/0.56	90.3	1,170		0.00(2)		

$x \lesssim 6.5$ where these relaxation effects enhance dT_c/dP by more than a factor of 10.[14]

It is important to realize that the presence of oxygen ordering effects in T_c implies that empty oxygen sites are present in the bulk sample. Analogous studies of the pressure dependence of J_c across single well-defined GBs would be expected to yield two important pieces of information regarding (1) the presence or absence of empty oxygen sites in the GB and (2) the intrinsic effect on J_c of compressing the GB region.

Previous ac susceptibility studies[20] on bulk polycrystalline samples of $YBa_2Cu_4O_8$ and $Tl_2CaBa_2Cu_2O_{8+\delta}$ indicated that the bulk J_c was enhanced through pressure, but it was not possible to extract detailed information; a comparably rapid increase in J_c was reported in early experiments on nearly optimally doped YBCO thin films.[21] For quantitative interpretation, studies of pressure-dependent effects involving a single well-defined GB are clearly needed. Such experiments have recently become possible with the availability of single [001]-tilt GB in bicrystalline rings of $YBa_2Cu_3O_x$ with varying misorientation angle θ and oxygen content x.[22] The ring geometry allows a more precise determination of J_c than the standard *I-V* technique since ring currents yield a very large magnetic moment, changes in which can be very sensitively detected in dc or ac susceptibility measurements. In addition, the magnetic susceptibility measurement does not require electrical contacts to the sample, as in transport measurements, which can lead to local heating effects.

In this paper we determine for a single [001]-tilt GB with a range of mismatch angles 0°–31° in bicrystalline YBCO rings the dependence of the critical current density $J_c = J_c(T,P,t)$ on temperature T, hydrostatic pressure P, and time t. We find that the critical current density J_c across GBs in both nearly optimally doped and underdoped bicrystals increases rapidly with hydrostatic pressure at the rate $d\ln J_c/dP \simeq +20$ to $+50$ % GPa^{-1} for most samples. This rate of increase is much more rapid than that expected from a simple GB model which assumes that the increase in J_c arises solely from the compression of the tunnel barrier with width W.

Significant pressure-induced relaxation effects are observed in J_c for all bicrystals, in addition to the intrinsic "nonrelaxation" contribution $(d\ln J_c/dP)_{\text{intr}}$. Importantly, the presence of sizeable relaxation effects in J_c signals the presence of vacant oxygen sites in the GB region. Filling these sites with additional oxygen anions would increase the hole carrier concentration and thus further enhance J_c across the GB. These results point to the importance for optimizing J_c to increase the oxygen concentration in the GB to as high a level as possible through Ca doping, annealing in high-pressure oxygen, or electro-transport techniques. In addition, it is found that compressing the GB region leads to a large intrinsic increase in the critical current density $(d\ln J_c/dP)_{\text{intr}} \simeq +15$ to $+25$ % GPa^{-1}. Results on one of the samples studied, ring *d* (see Table I), were published earlier.[23]

II. EXPERIMENT

Bicrystalline rings of superconducting $YBa_2Cu_3O_x$ with [001]-tilt GBs exhibiting mismatch angles θ between 0° and 31° were prepared for several different bulk oxygen concentrations x. See Table I for full information on the rings studied.

To obtain [001]-tilt GBs, pressed powder cylindrical samples were melt textured with two $SmBa_2Cu_3O_x$ single

crystal seeds placed on the top surface of the cylinders, with the crystal c axes aligned parallel to the cylinder axis. The seed crystals were rotated about their c axes so that a-b planes had the desired misorientation. Simultaneous seeding, initiated at the two crystals, leads to a melt textured "bicrystal" monolith with the desired [001]-tilt misorientation. Seeded bicrystal monoliths were prepared as cylinders with 10 or 26 mm diameters.[22] Disk wafers, 0.5–1 mm in thickness were cut, perpendicular to the c axis, from a bicrystal monolith. Generally, these wafers came from a depth of less than 5 mm from the seed, to minimize GB meander. Ring samples were then cut from the wafers, using a core drill (with abrasive slurry), such that the GB plane cut across the ring sample parallel to the ring axis. Typically, rings were prepared with $\sim 1 \times 1$ mm^2 cross section and ~ 5 mm outer diameter.

Measured values of J_c obtained from nominally identical, but independently prepared, samples commonly show a significant amount of scatter (see Fig. 7 below). Probably this results from imperfections in the GB, especially impurities, such as excess YBa_2CuO_5 (an insulating oxide comprising 25% of the starting powder mixture) that migrates along the growth front as solidification proceeds. Such impurities will be deposited at the intersection of growth fronts which originated at the two seeds, i.e., in the artificial GB. Thus one might expect that some (unknown and variable) fraction of the GB will not superconduct. In this paper, changes in the active region of the GB, resulting from the application of hydrostatic pressure, are examined.

Oxygen stoichiometries were fixed by processing the ring samples in a capped YBCO container placed in a furnace at a fixed temperature and O_2 partial pressure. The O_2 partial pressure was controlled by using a continuously monitored O_2/N_2 gas mixture flowing over the sample container as described in Ref. 24. Samples were held at temperature for 140 to 300 h and were then quenched into liquid nitrogen. The "optimally doped" samples were treated at 450 °C in flowing O_2. The flowing gas atmosphere for the $x=6.5$ ($x=6.4$) sample was 0.37% (0.13%) O_2 in N_2. Further details of the synthesis and preparation procedures are given elsewhere.[22]

Figure 1 shows the He-gas pressure cell (Unipress) made of hardened BeCu alloy which was used in the present studies to generate hydrostatic pressures to ~ 0.6 GPa. The Vespel sample holder containing the YBCO ring sample is positioned in the 7 mm dia bore of the pressure cell which has 2.8 cm OD and 11 cm length. Twelve copper electrical leads are brought into the lower part of the pressure cell through a conical seal, thus allowing, if desired, the simultaneous measurement of the electrical and magnetic properties of several samples simultaneously.

Two counterwound pickup coils, each 30 turns of 30 μm dia Cu wire, are wound on the Vespel sample holder (see Fig. 1) for the ac susceptibility measurement, one positioned around the YBCO ring, the other 2.3 mm below. Since primary ac (or dc) field amplitudes as high as 300 G are required in some experiments, internal heating effects are avoided by moving the primary coil from its normal location inside the pressure cell to outside the tailpiece of the cryostat. The primary coil is wound using 1.4 mm dia copper

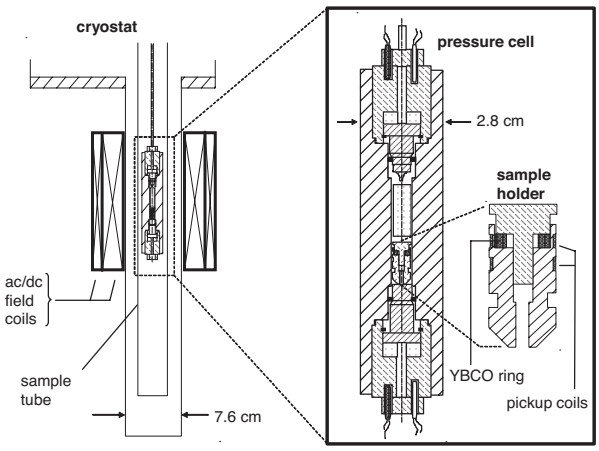

FIG. 1. (Right) He-gas BeCu pressure cell with 7 mm dia bore containing Vespel sample holder with YBCO bicrystalline ring and two counterwound pickup coils. In the top and bottom of cell are mounted two pairs of calibrated Ge and Pt thermometers. For temperature variation this cell is placed in sample chamber of a closed-cycle refrigerator (left). Two concentrically wound field coils are positioned outside cryostat tailpiece to generate ac or dc magnetic fields to ~500 G.

wire in the form of two independent solenoids. To ensure full penetration of the ac field to the sample through the cryostat tailpiece and pressure cell, the frequency of the ac field is reduced from its normal value of 1023 to only 1 Hz; at 10 Hz the reduction in the ac field amplitude at the sample, as determined by the kink temperature T_{kink} (see below), was found to be only 1%. The ac field is generated using a high-power bipolar power supply (Kepco BOP 72-6D) driven by an external oscillator. Standard ac susceptibility techniques are used with an SR 830 digital lock-in amplifier and SR 554 transformer preamplifier from Stanford Research Systems.

To vary the temperature over the range 5–300 K, the pressure cell is placed in the sample tube of a two-stage closed-cycle refrigerator (Balzers) with the BeCu capillary tube (3 mm OD $\times$ 0.3 mm ID) exiting out the top and connected to a three-stage He-gas compressor system (Harwood Engineering) at ambient temperature. Pressure is measured using a digital manganin gauge with absolute accuracy $\sim 1\%$ and resolution 1 bar at all pressures. The decrease in pressure upon cooling (typically less than 10% from 300 to 5 K) is minimized by placing an alumina cylinder in the cell bore (see Fig. 1) to reduce the volume of He in the cell to less than 0.5 cm^3 and by adding a 3.6 cm^3 He dead volume at ambient temperature outside the cryostat. Heaters on the second stage of the cryocooler and on the pressure cell allow excellent control of the cooling and warming rates. For precise measurements of T_c, for example, the cooling/warming rate is held at ~ 100 mK/min. To minimize temperature gradients, the second stage of the cryocooler is connected via a thick copper braid to a vertically slit copper tube surrounding the pressure cell, rather than to the bottom of the sample tube as in conventional cryocoolers. Two calibrated Ge (Lake Shore) and two platinum (Degussa) resistance thermometers are located on the top and bottom of the pressure cell (see Fig. 1).

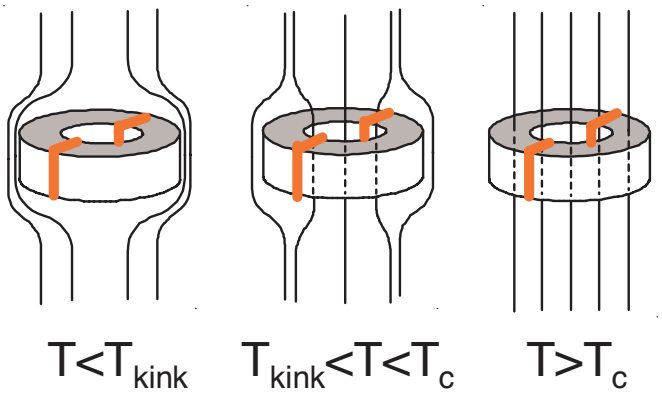

FIG. 2. (Color online) Illustration of flux lines from a magnetic field H applied perpendicular to the axis of a bicrystalline ring containing two GBs (red). From left to right: for temperatures $T < T_{\text{kink}}$ flux is excluded from ring, for $T_{\text{kink}} < T < T_c$ flux penetrates into center of ring, and for $T > T_c$ flux penetrates through entire ring.

At the above cooling/warming rates the temperature gradient across the 11 cm length of the pressure cell is typically less than 50 mK. Susceptibility data upon cooling or warming normally agree to within 15 mK. The pressure can be changed at any temperature above the melting curve of He which lies at 43.6 K for 0.6 GPa pressure; the ability to change pressure at low temperatures is essential when studying oxygen-ordering effects in the GBs or bulk of the high-T_c oxides. Care must be taken when cooling or warming through the liquid/solid transition of He; a technique introduced by Schirber[25] is used whereby a capillary heater maintains the temperature at the top of the cell approximately 2 K warmer than at the bottom while the temperature is slowly varied (50–100 mK/minute) through the melting temperature.

III. RESULTS OF EXPERIMENT

A. Ambient pressure studies

The critical current density J_c of a superconducting material is traditionally determined[2,3] in a current-voltage (I-V) experiment where the current I through a wire or thin bar-shaped sample with cross-sectional area A is increased until a finite voltage drop (typically $\sim 1\ \mu$V) is detected, thus defining the critical current I_c and the critical current density $J_c = I_c/A$. J_c is at its maximum value at 0 K, decreasing monotonically with increasing temperature. In this technique care must be taken to make low-resistance electrical contacts, a difficult problem with the high-T_c oxides.

An alternate technique, which offers a much more sensitive criteria for determining J_c and requires no current leads, is to apply a dc magnetic field H_{dc} at a fixed temperature $T < T_c$ to a superconducting ring (see Fig. 2), thus inducing a ring current I_{ring} proportional to H_{dc}, i.e., $I_{\text{ring}} = DH_{\text{dc}}$.[22] For a single-turn solenoid, D is equal to the solenoid diameter. Here we set D equal to the average of the inner and outer diameters of the ring; a more exact calculation[26] for the ring geometries used here would result in corrections to D of only a few percent. The current density is thus given by the expression $J_{\text{ring}} = A^{-1} I_{\text{ring}} = DA^{-1} H_{\text{dc}}$.

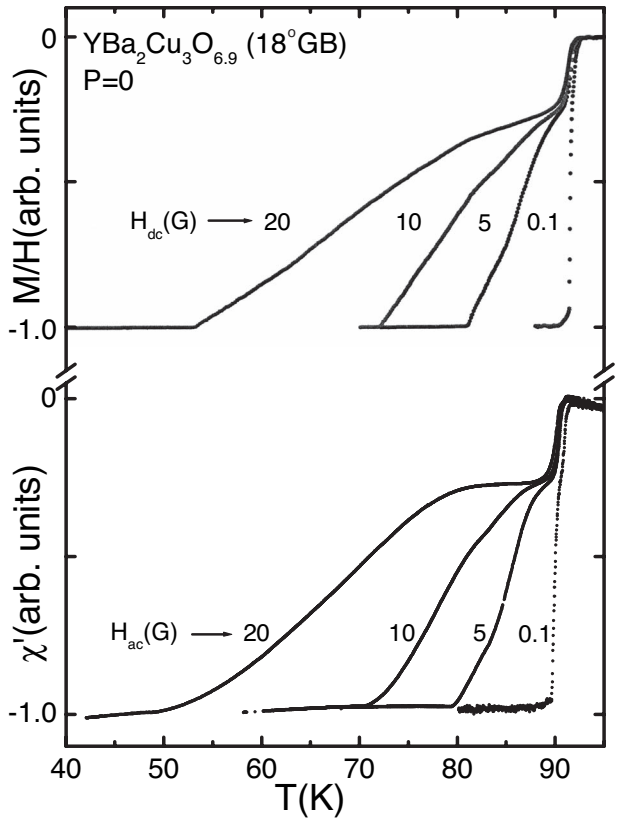

FIG. 3. Ambient pressure data comparing temperature-dependent (top) dc magnetic susceptibility M/H using a SQUID magnetometer to (bottom) real component of ac susceptibility $\chi'_{\text{ac}}(T)$ at field strengths $H_{\text{ac}} = H_{\text{dc}} = 0.1$, 5, 10, and 20 G on a single nearly optimally doped YBCO bicrystalline ring b with 18° GB.

Assume that a magnetic field H_{dc} is applied at a temperature T sufficiently low that J_{ring} is less than the critical current density $J_c(T)$. In this case the magnetic field generated by the ring current is equal and opposite to the applied field, thus preventing flux from entering the ring, as seen in Fig. 2 (left). The YBCO bicrystalline ring thus behaves as a perfect diamagnet, as evidenced by the large negative temperature-independent value of the zero-field-cooled (ZFC) dc magnetic susceptibility in Fig. 3 (upper) at low temperatures. If the temperature is now increased, J_{ring} remains constant but $J_c(T)$ decreases until at the kink temperature T_{kink}, where J_{ring} equals J_c, flux begins to penetrate into the ring interior through the weaker of the two grain boundaries, as illustrated in Fig. 2 (middle). For $H_{\text{dc}} = 20$ G this kink temperature lies at $T_{\text{kink}} = 52.5$ K where the temperature dependent susceptibility M/H exhibits a sharp break or "kink" and begins to rise steeply, as seen in Fig. 3 (upper). As the temperature increases beyond T_{kink}, more and more flux enters into the ring interior until finally, when the small plateau in M/H immediately below T_c is reached, flux has fully penetrated into the interior of the ring (Fig. 2, middle). A further increase in temperature to $T > T_c$ results in the ring entering the normal state where magnetic flux fully penetrates through the ring material, as illustrated in Fig. 2 (right).

As seen in Fig. 3 (upper), if a weaker magnetic field H_{dc} than 20 G is applied at low temperatures, say 10, 5, or 0.1 G, the ring current decreases correspondingly and thus T_{kink} shifts to progressively higher temperatures, reflecting the decrease in $J_c(T)$ with increasing temperature. In a dc measurement, therefore, the temperature dependence of the critical current density $J_c(T)$ can be readily determined from the change in T_{kink} as a function of the applied field H_{dc}.

Unfortunately, dc susceptibility studies are not easily compatible with He-gas hydrostatic pressure technology, although possible.[27] In the present high-pressure experiments, we utilize ac susceptibility measurements to determine $J_c(T)$ for a given YBCO bicrystalline ring. As seen in Fig. 3 (bottom) oscillatory ac fields $H(t)=H_{ac}\cos\omega t$ with amplitudes $H_{ac}=20$, 10, 5, and 0.1 G at 1 Hz are applied by the external primary field coils (see Fig. 1) to the ring sample mounted in the pressure cell, thus inducing superconducting ring currents $I(t)=I_{ac}\sin\omega t$. For the same ac field amplitudes as in the dc experiments, $H_{ac}=H_{dc}$, the values of the kink temperatures T_{kink} are seen in Fig. 3 to be quite close. The good agreement between ac and dc susceptibility determinations of J_c was previously demonstrated by Herzog *et al.*[28] We note that in the ac measurement the value of T_{kink} is the same whether the experiment is carried out in the field-cooled or zero-field-cooled mode.

For temperatures below T_{kink}, the oscillatory magnetic field generated by these ac ring currents is equal and opposite to the applied ac field, thus preventing flux from entering the ring. As the temperature is increased above T_{kink}, however, the ring current amplitude I_{ac} exceeds the critical current I_c and magnetic flux begins to flow in and out of the ring twice each period through the weaker of the two grain boundaries when $\sin\omega t \simeq \pm 1$. In Fig. 3 one notices that at the higher field amplitudes, the "kink" in $\chi'_{ac}(T)$ becomes noticeably more rounded than that in the dc measurement, making a precise determination of T_{kink} difficult. Fortunately, as seen in Fig. 4, the imaginary part of the ac susceptibility, $\chi''_{ac}(T)$, retains its sharp kink, allowing an accurate determination of T_{kink} even at higher field amplitudes. An alternate method to determine $J_c(T)$ is to fix the temperature at a value $T<T_c$ and vary H_{ac} until a kink occurs.

In Fig. 5 the temperature dependence of the ac susceptibility $\chi'_{ac}(T)$ is plotted for a nearly optimally doped YBCO ring with a low-angle 4° GB for values of H_{ac} from 1 to 250 G. Much higher magnetic field amplitudes are necessary to shift T_{kink} here than for the above ring with 18° GB since the values of J_c are much higher in the former. The values of T_{kink} from $\chi''_{ac}(T)$ are listed in the caption to Fig. 5; in the figure itself vertical arrows mark T_{kink} for the four lowest values of H_{ac}.

In analogy to the dc experiment, the temperature dependence of the critical current density for $T=T_{kink}$ is given by the expression $J_c(T)=A^{-1}I_{ac}(T)=DA^{-1}H_{ac}(T)$. In Fig. 6 we display $J_c(T)$ determined in this way taken from the ac susceptibility data in Figs. 3–5 on the nearly optimally doped YBCO bicrystalline rings with 4° and 18° GBs. Included in Fig. 6 are also all $J_c(T)$ dependences obtained in the present ac susceptibility studies on nearly optimally doped YBCO bicrystalline rings with various mismatch angles θ from 0° to

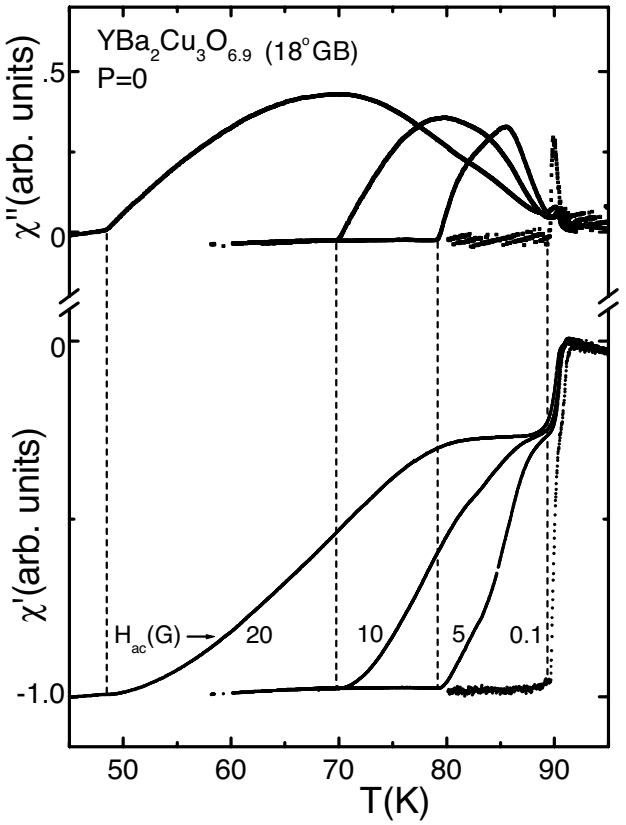

FIG. 4. Comparison of real $\chi'_{ac}(T)$ and imaginary $\chi''_{ac}(T)$ parts of ac susceptibility versus temperature for a nearly optimally doped YBCO bicrystalline ring *b* with 18° GB at ac field amplitudes $H_{ac}=0.1$, 5, 10, and 20 G. The corresponding kink temperatures $T_{kink}=89.6$, 79.1, 69.8, and 48.5 K can be most accurately determined from $\chi''_{ac}(T)$ and are marked by vertical dashed lines. T_{kink} marks the temperature where magnetic flux first begins to enter the ring on warming (see illustration in Fig. 2).

31°. The solid lines in Fig. 6 are fits to the data using the following expression valid near T_c (Ref. 29)

$$J_c(T) = J_c(0)[1 - T/T_c]^{\beta}, \tag{1}$$

where the values of the fit parameters $J_c(0)$ and β are given in Table I. Note that the $J_c(T)$ dependences for the rings with 21° and 31° GBs appear to lie anomalously low. The GBs in these rings appear to be of somewhat inferior quality, possibly due to an unusually high concentration of GB defects such as oxygen vacancies.

In Fig. 7 the values of J_c at 77 K in the present experiment on nearly optimally doped YBCO rings, obtained by extrapolation of the data in Fig. 6, are compared on a logarithmic scale to those from dc magnetization studies by Veal *et al.*[30] on nearly optimally doped melt-textured bicrystalline rings as well as from earlier *I-V* experiments on melt-textured YBCO specimens.[31] The relatively high values of J_c for the *I-V* experiments may be at least in part due to the use of a much less sensitive criterion for J_c than in the present magnetization studies. In all experiments J_c is found to fall off rapidly as the GB mismatch angle θ is increased.

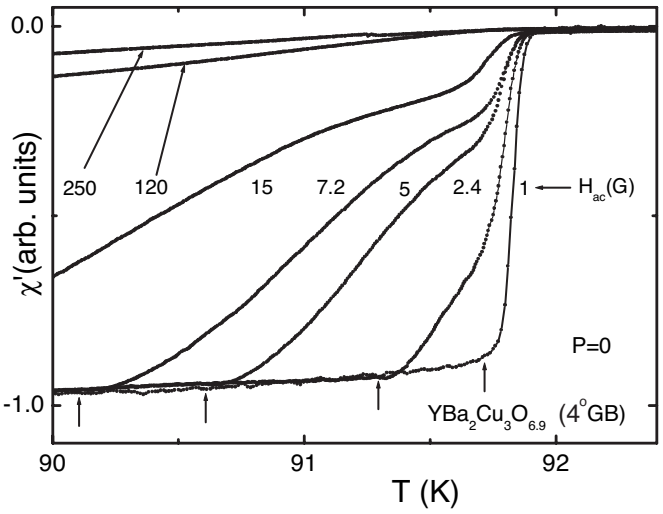

FIG. 5. Real part $\chi'_{ac}(T)$ of ac susceptibility for field amplitudes H_{ac}=1, 2.4, 5, 7.2, 15, 120, and 250 G for a nearly optimally doped YBCO bicrystalline ring a' with 4° GB. The corresponding kink temperatures from $\chi''_{ac}(T)$ are T_{kink}=91.75, 91.31, 90.62, 90.11, 88.67, 74.5, and 64.2 K.

Underdoped YBCO samples are synthesized by annealing in low oxygen partial pressure at elevated temperatures, thus drawing oxygen anions out of both the bulk and the GBs in bicrystalline rings.[22] As a result, it would be anticipated that both T_c and J_c will take on reduced values in underdoped YBCO rings. In Fig. 8 we plot for a ring with a 12° GB both T_c and J_c versus the oxygen concentration x in the bulk. As was also observed in thin film samples,[32] whereas T_c versus x is seen to pass through a maximum at optimal bulk doping ($x \simeq 6.95$), $J_c(x)$ increases monotonically with x up to the maximum bulk concentration $x \simeq 6.98$. It is important to note that the oxygen concentration in the GB region likely differs from that in the bulk. Since the bulk chain sites are empty for x=6 and full for x=7, these sites for x=6.98 are 98% filled with oxygen. Recent experiments indicate that the degree of occupation of the oxygen sites in the GB may be a good deal lower, but the technique is difficult to apply in general.[8,9] Note that in Fig. 8 J_c increases monotonically with x for both 12° and 28° GBs, indicating that higher values of J_c can likely be achieved if the GB is fully oxygenated. It would obviously be advantageous to develop a method to estimate the concentration of vacant oxygen sites in the GB which are accessible to mobile oxygen anions. Below we introduce just such a technique.

Reducing the bulk oxygen concentration x below the level shown in Fig. 8 leads to particularly sharp reductions in both the bulk T_c value and the J_c value across the GB. In Fig. 9 (lower) T_{kink} for a strongly underdoped $YBa_2Cu_3O_{6.4}$ bicrystalline ring with 20° GB is seen to shift rapidly to lower temperatures upon the application of only very small ac field amplitudes of 0.03, 0.1, 0.54, and 1.1 G. The estimated J_c values for this and further underdoped rings with various GB angles are seen in Fig. 10 to be an order of magnitude lower than those in Fig. 6 for nearly optimally doped YBCO (see also Table I).

Of particular interest in the $\chi'_{ac}(T)$ data in Fig. 9 (lower) is the presence of a sizeable plateau between 40 and 50 K

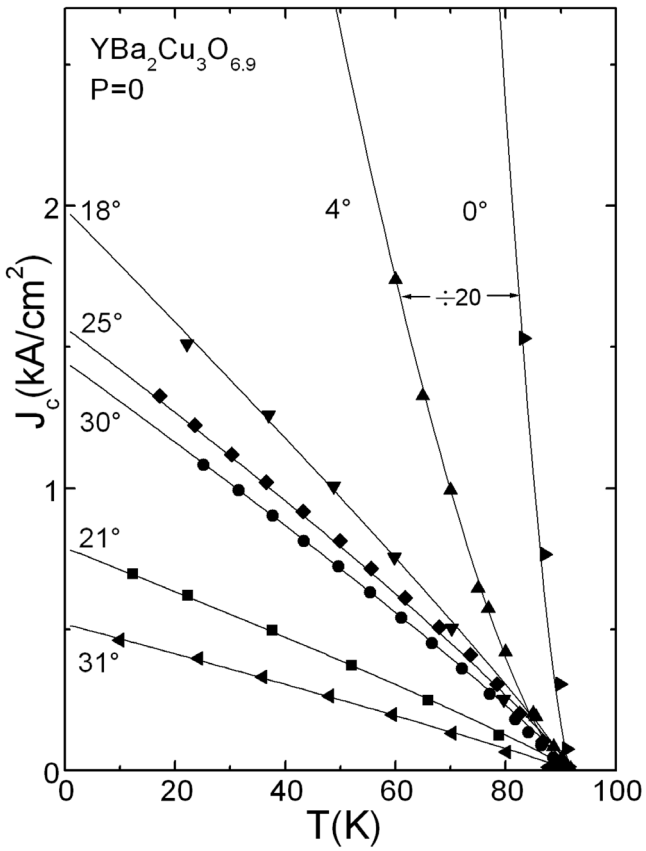

FIG. 6. Calculated critical current density $J_c(T)$ versus temperature from ac susceptibility data on nearly optimally doped YBCO bicrystalline rings (counterclockwise m, a', b, d, e, c, g) for seven different GB mismatch angles θ. The $J_c(T)$ values for the 0° and 4° GB rings have been reduced twentyfold. Solid lines are fits to data using Eq. (1) with fit parameters $J_c(0)$ and β given in Table I.

which, unlike the data for the nearly optimally doped rings in Figs. 3–5, does not vanish at very low H_{ac} field amplitudes. To establish whether this wide plateau might arise from small residual magnetic fields in the cryostat, which were measured with a Hall probe to be ~0.2–0.5 G, a dc field of 0.5 G was applied both parallel and perpendicular to the ring axis. This field resulted in only a tiny 0.15 K shift in T_{kink}, a value far smaller than the 12 K plateau width. In addition, reducing the ac field amplitude from 0.1 to 0.03 G led to no measurable reduction in the plateau width, as seen in Fig. 9 (lower). This suggests that the plateau in $\chi'_{ac}(T)$ for the strongly underdoped $YBa_2Cu_3O_{6.4}$ ring is an intrinsic property and signals that the GB J_c goes to zero at temperatures well below the bulk T_c value. Similar effects are found in the other three underdoped YBCO rings studied here as well as for thin-film bicrystals.[33]

B. High pressure studies

1. Pressure dependence of $J_c(T)$

In Fig. 11 (left) we show the temperature dependence of the real part of the ac susceptibility at 0 and 0.60 GPa pressure for a nearly optimally doped YBCO bicrystal with 30°

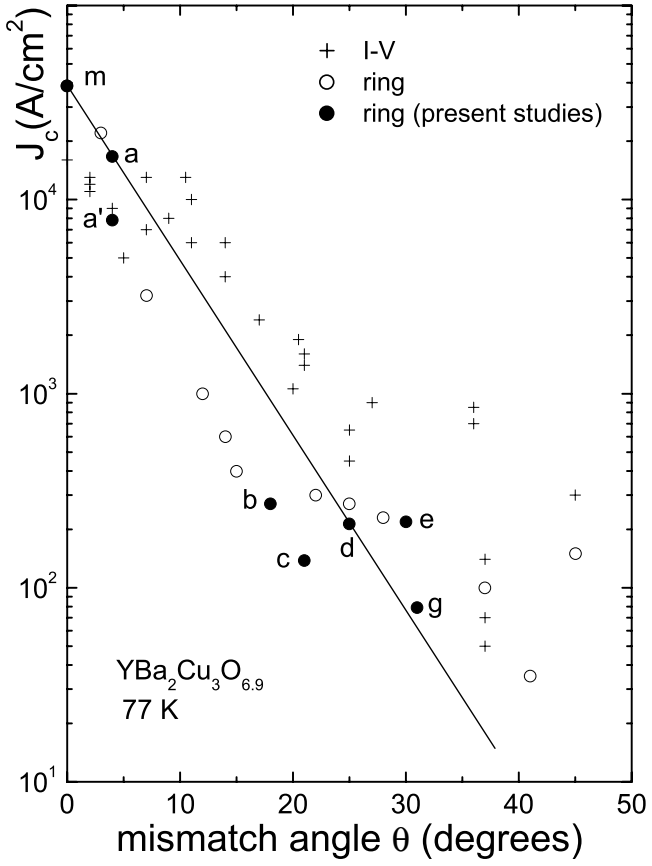

FIG. 7. Critical current density J_c at 77 K on logarithmic scale as a function of GB mismatch angle θ for nearly optimally doped melt-textured YBCO rings: (●) present studies, (○) previous (Ref. 30) magnetic susceptibility measurements, (+) *I-V* measurements (Ref. 31). Straight line through data given by expression: $J_c(T) = J_c(0)\exp[-\theta/\theta_0]$, where $J_c(0) = 4\times10^4$ A/cm^2 and $\theta_0 = 4.8°$. Lower-case letters label rings in present studies (see Table I).

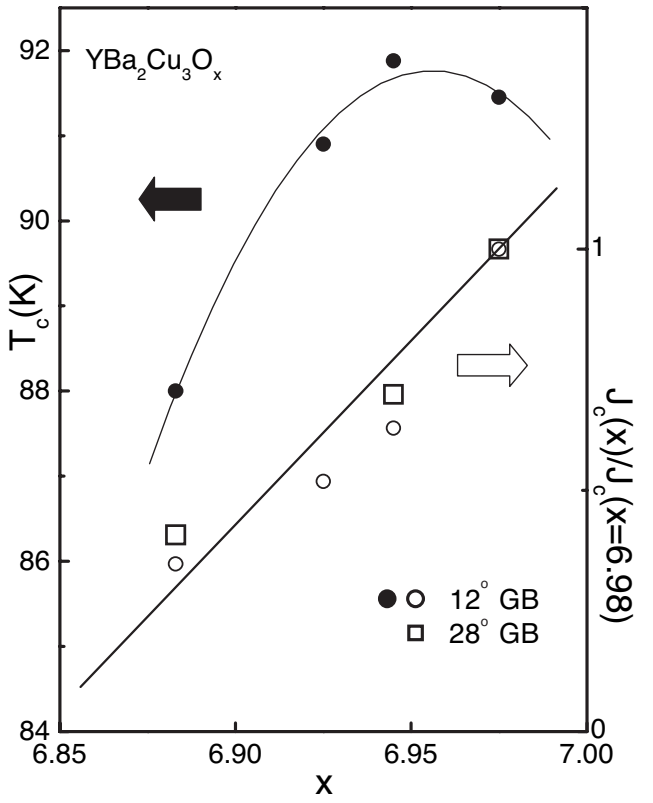

FIG. 8. Superconducting transition temperature $T_c(x)$ and relative critical current density $[J_c(x)/J_c(6.98)]$ at 77 K versus bulk oxygen content x for $YBa_2Cu_3O_x$ bicrystals with 12° and 28° GBs. Whereas $T_c(x)$ passes through a maximum near $x=6.95$, $J_c(x)$ increases monotonically with x. Solid lines are guide to eye.

GB. T_{kink} is seen to shift to higher temperatures under pressure; the data indicate that J_c increases with pressure at the rapid rate $d\ln J_c/dP \simeq +0.26$ GPa^{-1}. This is brought out clearly in Fig. 11 (right) where $J_c(T)$ is plotted versus temperature for three different pressures. The solid lines are fits to the data using Eq. (1); the values of $J_c(0)$ and β obtained from the fits are given in Table I. That J_c increases rapidly with pressure at all temperatures is illustrated in Fig. 12 where it is seen that the data at both pressures coalesce onto one curve when $J_c(T)/J_c(0)$ is plotted versus temperature. In contrast to the rapid increase of J_c, the superconducting transition temperature at $T_c \simeq 92$ K increases only slightly with pressure $d\ln T_c/dP \approx +0.0024$ GPa^{-1}, as seen in Fig. 11 (left).

In Fig. 13 $J_c(T)$ is seen to increase rapidly with pressure ($d\ln J_c/dP \simeq 0.30$ and 0.32 GPa^{-1}, respectively) for nearly optimally doped YBCO bicrystals with 18° and 21° GBs. Our measurements in Fig. 9 (upper) on the underdoped $YBa_2Cu_3O_{6.4}$ ring with 20° GB reveal an even more rapid increase in J_c with pressure ($d\ln J_c/dP \simeq 0.60$ GPa^{-1}). In fact, a rapid increase in J_c with pressure is found for *all* bicrystalline YBCO rings studied with differing mismatch angles $\theta > 0°$ and oxygen concentrations x, as seen in Table I. Since $J_c(T) = DA^{-1}H_{ac}(T)$, the slight change in the ring geometry under pressure[34] leads to small correction in $d\ln J_c/dP$; we ignore this correction since it is approximately two orders of magnitude less than the measured values above.

To investigate whether the rapid increase in J_c under pressure arises from the GB itself or from the melt-textured bulk material in the YBCO ring, $J_c(T)$ was also determined for two nearly optimally doped melt-textured YBCO rings with *no* artificial GB ($\theta = 0°$). The data for ring *m* at ambient pressure are shown in both Figs. 6 and 14. The solid line through the data in Fig. 14 is a fit using the following formula from Ginzburg-Landau theory:[35]

$$J_c = J_c(0)\left[1-\left(\frac{T}{T_c}\right)^2\right]\left[1-\left(\frac{T}{T_c}\right)^4\right]^{1/2}, \qquad (2)$$

resulting in the rough estimate $J_c(0) \approx 275$ kA/cm^2. From the data in Fig. 14 it can be estimated that J_c is independent of hydrostatic pressure, i.e., $|d\ln J_c/dP| \leq 0.02$ GPa^{-1}; the independence of J_c on pressure was confirmed in a parallel experiment on a slightly underdoped $YBa_2Cu_3O_{6.86}$ ring m' with no GB. This result demonstrates that the origin of the rapid increase observed in $J_c(T)$ under pressure arises from

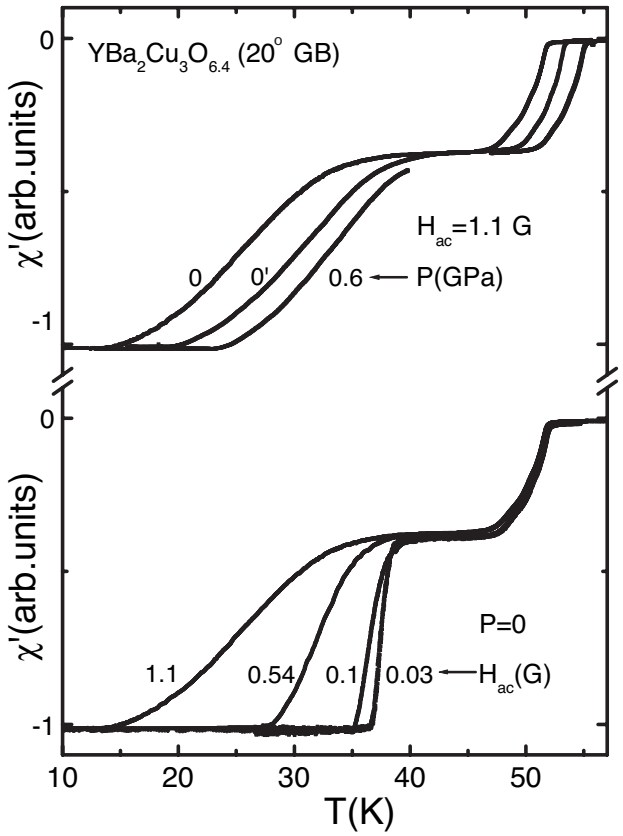

FIG. 9. Real part $\chi'_{ac}(T)$ of the ac susceptibility for an underdoped YBCO bicrystalline ring k with 20° GB (lower) for field amplitudes H_{ac}=0.03, 0.1, 0.54, and 1.1 G. (upper) Dependence of $\chi'_{ac}(T)$ at H_{ac}=1.1 G for 0 GPa, 0.60 GPa pressure applied at RT, but released at 60 K (0′ GPa). The missing data points near 45 K for 0.60 GPa come from the disturbance of the measurement as the sample is cooled through the freezing point of the He pressure medium.

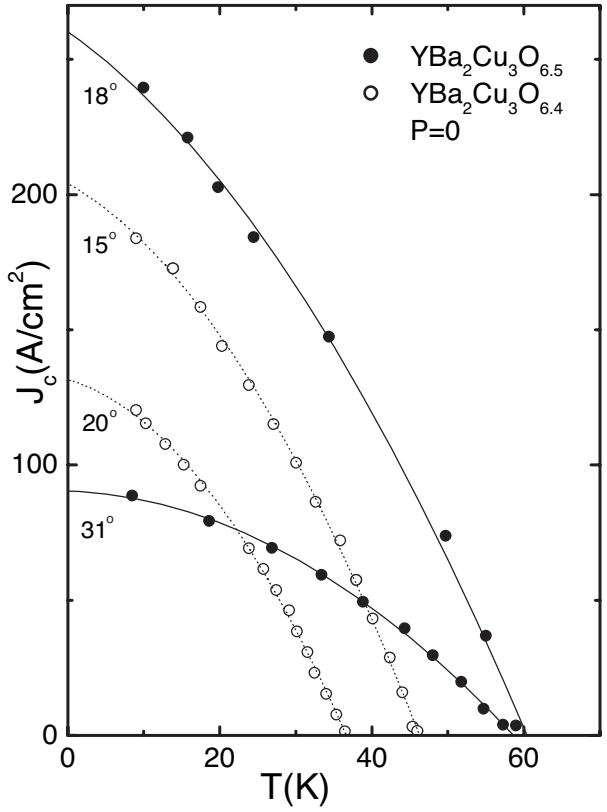

FIG. 10. Critical current density J_c versus temperature at ambient pressure for strongly underdoped YBCO rings (b'', g'', i, k) with x=6.5 and 6.4 and various mismatch angles. Lines are fits to data using Eq. (1) with parameters ($J_c(0)$ and β) given in Table I.

changes in the properties of the GB itself rather than in the ring's bulk properties.

In Fig. 15 is displayed the effect of the application at temperatures above T_c of an additional dc magnetic field of 120 G on the temperature and pressure dependence of $J_c(T,P)$ for a nearly optimally doped YBCO ring. Note that under the dc field the temperature dependence $J_c(T)$ assumes a positive curvature both under ambient and high pressure. As reported in Ref. 23, we find in the absence of a dc field $d \ln J_c/dP \simeq +0.20$ GPa^{-1}, whereas for H_{dc}=120 G the critical current density increases under pressure at the somewhat more rapid rate $d \ln J_c/dP \simeq +0.26$ GPa^{-1}.

2. Relaxation effects in $J_c(T,P)$

As discussed in the Introduction, vacant oxygen sites in the GB region open the door for oxygen ordering effects in J_c. Such relaxation behavior in J_c can be easily identified by determining whether or not the pressure dependence of J_c depends on the temperature at which the pressure is changed. With the sole exception of the 0′ data in Fig. 9 (upper), the pressure was changed at ambient temperature for all data presented thus far. Significant pressure-induced oxygen ordering effects in the CuO chains in bulk YBCO, particularly in the underdoped samples, were uncovered by noting that the pressure dependence of $T_c(P)$ depends markedly on the temperature at which the pressure is changed.[13,14]

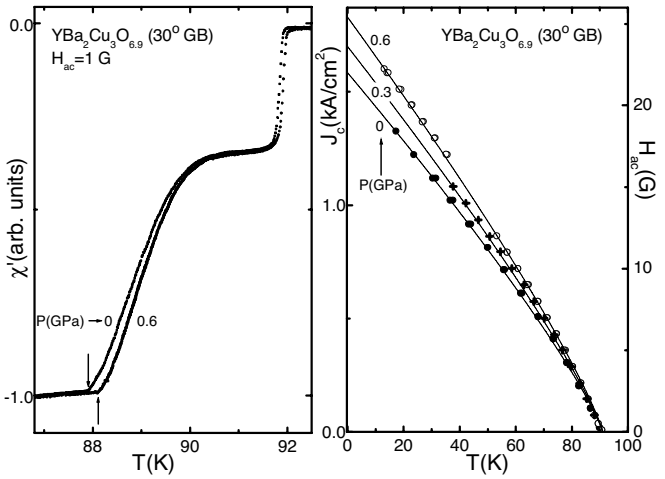

FIG. 11. (left) Real part of the ac susceptibility versus temperature for nearly optimally doped YBCO ring e with 30° GB at 0 and 0.60 GPa pressure. (right) Temperature dependence of critical current density J_c calculated from ac susceptibility at different field amplitudes H_{ac} for pressures of 0, 0.3 and 0.6 GPa. At all temperatures J_c is seen to increase rapidly with pressure.

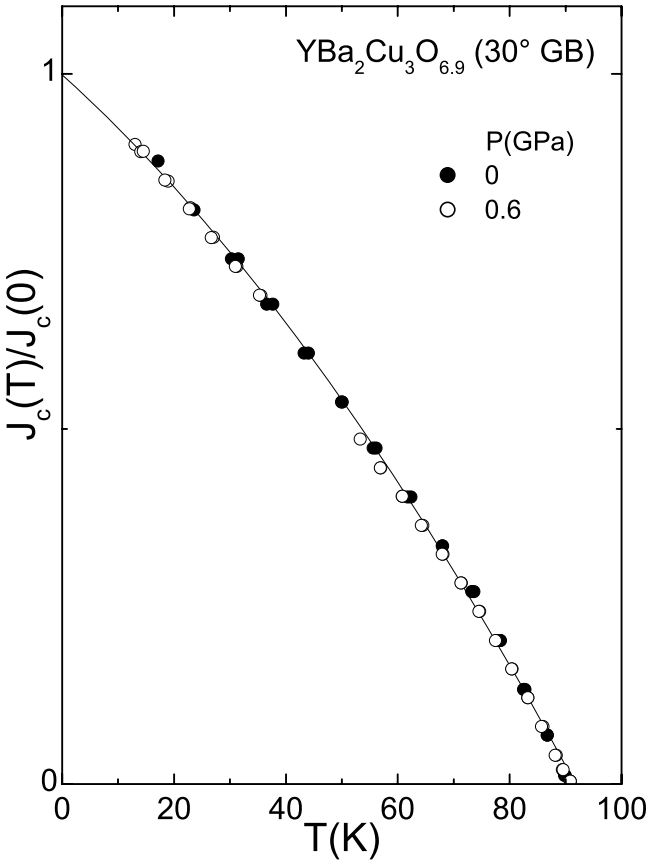

FIG. 12. Relative temperature dependence of critical current density $J_c(T)/J_c(0)$ for nearly optimally doped YBCO ring *e* with 30° GB at 0 and 0.60 GPa pressures. The overlap of the data demonstrates that J_c increases with hydrostatic pressure an equal amount (+26 % GPa^{-1}) for all temperatures below T_c.

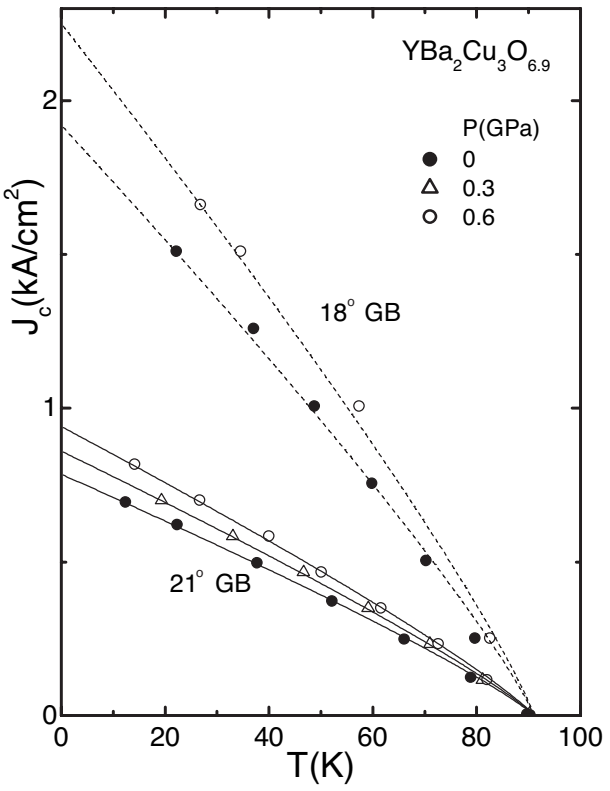

FIG. 13. Temperature dependence of critical current density J_c for nearly optimally doped YBCO rings (*b* and *c*) with 18° and 21° GBs at different hydrostatic pressures. J_c increases rapidly with pressure for both rings. Lines are fits to data using Eq. (1) with parameters [$J_c(0)$ and α] for ambient pressure given in Table I.

In Fig. 16 (upper) it is seen that the application of 0.6 GPa pressure at 295 K to an underdoped $YBa_2Cu_3O_{6.4}$ ring with 20° GB leads to an increase in J_c(9 K) from 122 to 165 A/cm^2 (point 1 to point 2). If the pressure is now released at temperatures of 50 K and below, J_c(9 K) is seen to *not* decrease back fully to its initial value at point 1, but rather to hang up at the much higher value of 150 A/cm^2 (point 3). At these low temperatures the oxygen anions are frozen in place so that they are unable to relax back to their initial positions when the pressure is released. If the ring sample is now annealed for $\frac{1}{2}$ h at temperatures T_a=100 K and above, J_c(9 K) is seen to remain essentially constant until the annealing temperature T_a climbs above 200 K. Finally, at T_a =295 K (point 11) significant relaxation in J_c(9 K) becomes evident. If the ring is now annealed at the fixed temperature 295 K for extended periods of time, J_c(9 K) is seen to relax further (points 11–18) towards its initial value at point 1. The fraction of the pressure-induced enhancement in J_c due to relaxation effects is thus given by $\eta \simeq (150-122)-(165-122)=0.65$.

The time dependence of J_c in this experiment is illustrated in Fig. 16 (lower). The relaxation time τ for this GB relaxation process can be estimated by fitting the time-dependent data using the equation

$$J_c(t) = J_c(\infty) - [J_c(\infty) - J_c(0)]\exp\{-(t/\tau)^{\alpha}\}, \qquad (3)$$

where $J_c(0)$ and $J_c(\infty)$ are the initial (point 3) and fully relaxed (point 1) values of the critical current density, respectively. From the best fit to the data, the estimated GB relaxation time is $\tau \simeq 9$ h with $\alpha \simeq 0.34$. Using the Arrhenius law $\tau=\tau_0 \exp[E_a/k_BT]$, the activation energy is estimated to be $E_a \simeq 0.96$ eV, where we set $\tau_0 \simeq 1.4\times10^{-12}$ s from previous studies.[11]

The relaxation of the superconducting transition T_c for this sample was measured in the same experiment and analyzed using Eq. (3) with T_c substituted for J_c. The results are plotted in Fig. 17 for both $J_c(t)$ and $T_c(t)$. Inspection of the data in this graph tells us immediately that the relaxation in $J_c(t)$ is more rapid than that in $T_c(t)$. This is consistent with the fact that oxygen diffusion in the GB region is more rapid than in the bulk.[36] From the best fit to the $T_c(t)$ data using Eq. (3), $\tau \simeq 21$ h, $\alpha \simeq 0.5$, and $E_a \simeq 0.98$ eV are obtained; the relaxation time for the bulk property $T_c(t)$ is thus more than twice as long as that for the GB property $J_c(t)$.

We now search for pressure-induced relaxation phenomena in $J_c(T)$ in a second sample, a nearly optimally doped YBCO bicrystal with 25° GB. Less prominent relaxation effects in J_c are anticipated than for the previous sample since the bulk material, and likely the GB region, is much more

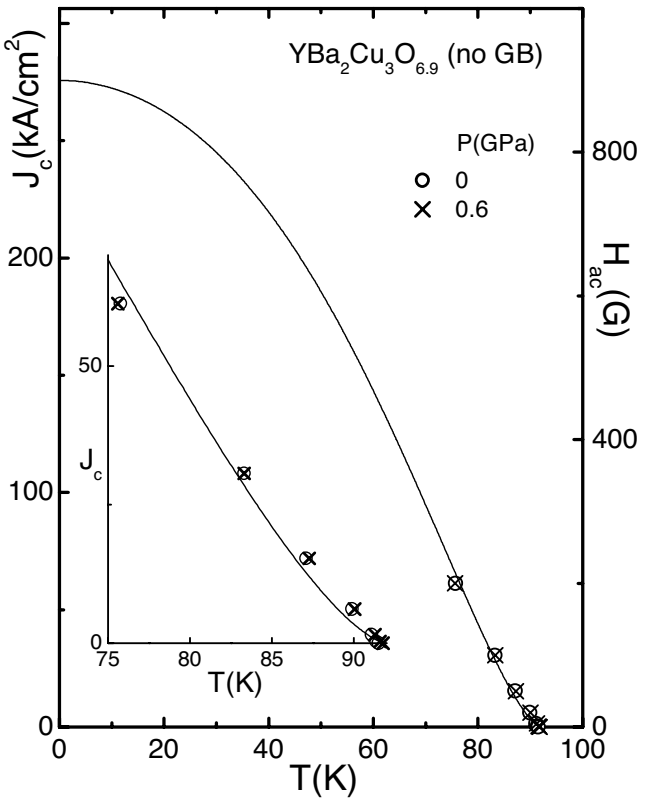

FIG. 14. Temperature dependence of critical current density J_c and corresponding field amplitude H_{ac} for nearly optimally doped YBCO ring *m* with no GB (θ=0°) at hydrostatic pressures 0 and 0.6 GPa. J_c is seen to not change with pressure. Line is fit to data using Eq. (2).

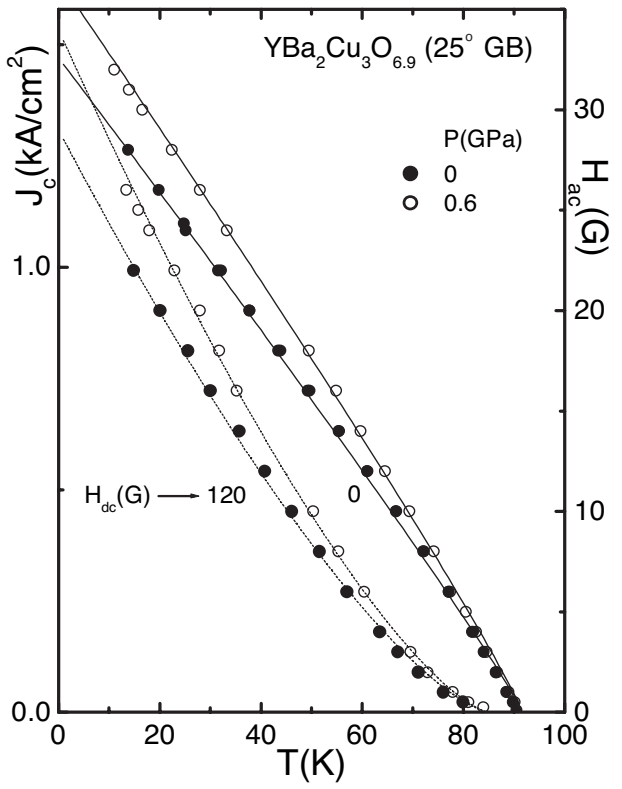

FIG. 15. Temperature dependence of critical current density J_c and corresponding field amplitude H_{ac} for nearly optimally doped YBCO ring *d* with 25° GB at hydrostatic pressures 0 and 0.6 GPa and dc field values 0 and 120 G. Fits to data using Eq. (1) are given by solid lines ($\beta \simeq 0.87$) and dashed lines ($\beta \simeq 1.4$).

heavily oxygenated and thus has far fewer vacant oxygen sites.

In Fig. 18 (upper) one sees that the application of 0.60 GPa pressure at 290 K prompts J_c at 9 K to increase from 1.291 to 1.447 kA/cm^2 (point 1 to point 2). If the pressure is then released at temperatures below 50 K to point 3, J_c does *not* decrease back to its initial value J_c =1.291 kA/cm^2, but rather to 1.322 kA/cm^2, a value 0.031 kA/cm^2 higher, implying the relaxation fraction $\eta \simeq (1.322-1.291)(1.447-1.291)=0.20$. Remeasuring J_c after annealing the sample for $\frac{1}{2}$ h at successively higher temperatures results in no change in J_c until the annealing temperature reaches values $T_a > 250$ K whereupon J_c relaxes back to its initial value (points 1 and 11). In a subsequent experiment shown in Fig. 18 (lower), the relaxation time τ for this GB relaxation process is estimated by annealing for different lengths of time at a fixed temperature (270 K) following pressure release at low temperatures. The value of J_c at 9 K is seen to show an exponential relaxation behavior. From the best fit to the data using Eq. (2), the estimated GB relaxation time is $\tau \simeq 5.9$ h for $\alpha \simeq 0.34$ and $E_a \simeq 0.87$ eV. As expected, the relaxation effects are much smaller ($\eta \simeq 0.20$) for this nearly optimally doped sample *d* than for the underdoped sample *k* above where $\eta \simeq 0.65$. The results of relaxation measurements on three further YBCO rings (a',*b*,*e*) are given in Table I (for ring *e* the value $\eta > 0.13$ is listed since in this measurement insufficient time elapsed after applying pressure at room temperature for full relaxation to occur).

That the relaxation in J_c indeed results from the motion of oxygen anions in the GB region is supported by two experimental findings: (1) the relaxation in J_c occurs in the same temperature region (250–290 K), where oxygen ordering phenomena in bulk YBCO are known to occur,[13,14,16] and (2) as seen in Fig. 16 and Table I, the magnitude of the relaxation effects in J_c increases substantially in underdoped (underoxgenated) YBCO bicrystals where the concentration of empty oxygen sites is much higher, thus opening up many more oxygen relaxation channels.

IV. DISCUSSION

The values of both the critical current density J_c at 9 K and its relative pressure derivative $d \ln J_c/dP$ versus mismatch angle θ are plotted in Fig. 19 for all YBCO bicrystalline rings studied in the present experiments. In addition to the general decrease in J_c with increasing θ, it is seen that J_c is significantly smaller for the underdoped than for the nearly optimally doped samples. Two possible reasons for this latter result are (1) underdoped YBCO samples have lower values of T_c which would tend to lead to lower J_c's and (2) underdoped YBCO samples, which are underoxygenated in the bulk, likely exhibit sizeable oxygen depletion in the GB re-

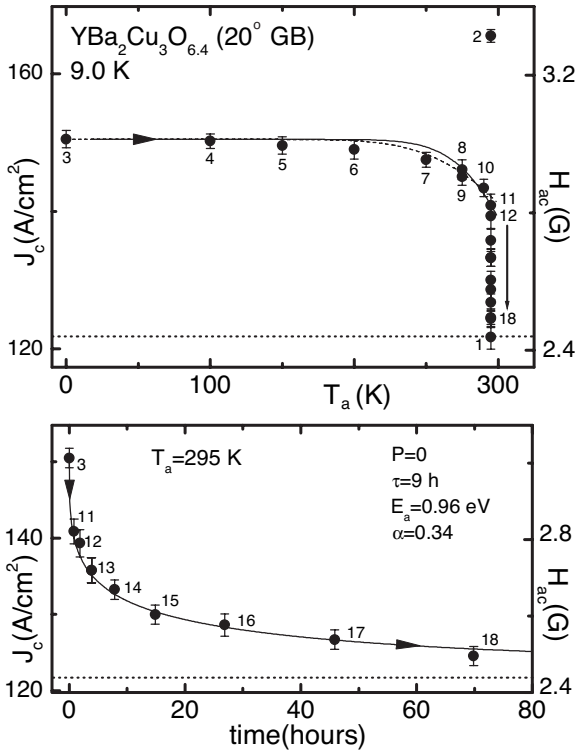

FIG. 16. For strongly underdoped $YBa_2Cu_3O_{6.4}$ bicrystalline ring k with 20° GB: (upper) dependence of critical current density J_c at 9 K on annealing temperature T_a. Numbers give order of measurement. Solid and dashed lines through data are guides to the eye. Horizontal dotted line marks initial value of J_c(9 K) at point 1. (lower) Dependence of J_c on time for fixed annealing temperature T_a=295 K following release of pressure at temperatures less than 50 K. Solid line is fit to data using Eq. (3) giving values of parameters listed. Horizontal dotted line in both graphs marks initial value of J_c(9 K) at point 1.

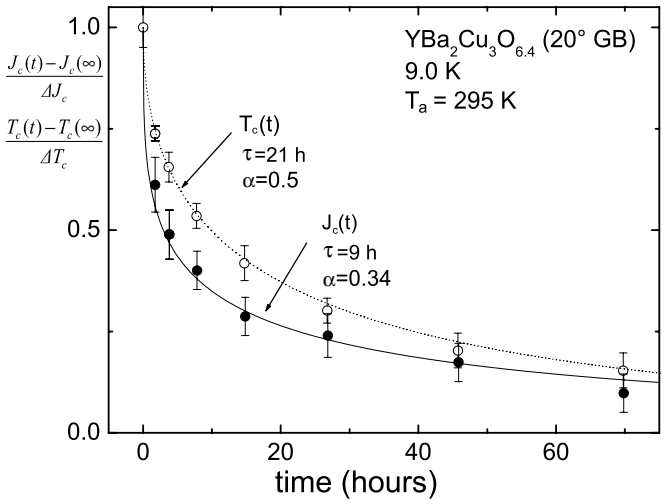

FIG. 17. Comparison of the relative dependences of the critical current density $J_c(t)$ at 9 K and the superconducting transition temperature $T_c(t)$ on the annealing time at T_a=295 K for $YBa_2Cu_3O_{6.4}$ bicrystalline ring k with 20° GB following the release of pressure at low temperatures. $J_c(\infty)$ and $T_c(\infty)$ are the respective values after infinite time. $\Delta J_c \equiv J_c(0) - J_c(\infty)$ and $\Delta T_c \equiv T_c(0) - T_c(\infty)$, all quantities as used in Eq. (3). $J_c(t)$ relaxes more than twice as fast as $T_c(t)$.

gion, leading to a lower carrier concentration compatible with only relatively weak supercurrents.

As seen in Fig. 19 (lower), for nearly optimally doped samples the relative pressure derivative does not show any systematic change with mismatch angle θ, most values lying between 0.2 and 0.35 GPa^{-1}. Two particularly large values of $d \ln J_c/dP$ are found for the strongly underdoped rings i and k; as discussed below, this is likely the result of strong relaxation effects due to the relatively large number of empty oxygen sites in their GBs. A good deal of scatter is seen in the values of both J_c and $d \ln J_c/dP$ in Fig. 19, evidently the result of differences in the quality of the GB region. Note, for example, that both J_c and $d \ln J_c/dP$ lie lower for sample b' than for sample b, whereas both quantities are nearly the same for samples g' and g.

The rapid increase in J_c under pressure suggests that J_c can be further increased at ambient pressure by compressing textured YBCO material through suitable chemical procedures. How much compression would be necessary? The relative change in J_c with GB width W is given by $d \ln J_c/d \ln W = -\kappa_{GB}^{-1}(d \ln J_c/dP)$, where $\kappa_{GB} \equiv -d \ln W/dP$ is the compressibility of the GB. If we assume to a rough first approximation that κ_{GB} is comparable with the average linear compressibility of YBCO in the CuO_2 plane,[37] $\kappa_a \equiv -d \ln a/dP$, where a is an in-plane lattice parameter and $\kappa_a \approx 2 \times 10^{-3}$ GPa^{-1},[34] it follows that $d \ln J_c/d \ln W \approx -100$ to -200. This implies that J_c increases under pressure at a rate which is 100× to 200× more rapid than the decrease in GB width. Compressing the GB by 10% should, therefore, lead to a tenfold enhancement in J_c. Lattice compression of thin films by a few % can be readily achieved through epitaxial growth techniques.[38]

We now examine the question of the mechanism behind the strong enhancement in J_c as the GB is compressed ($d \ln J_c/dP \approx 0.2$ to 0.4 GPa^{-1}). High pressures may modify the GB in a number of different ways, including (1) compression of the GB region, (2) intrinsic change in carrier concentration,[12,15] (3) pressure-induced oxygen-ordering effects in the GB with accompanying changes in carrier concentration, in analogy with the well studied pressure-induced oxygen ordering effects in the bulk,[12–14,16] and (4) change in the value of T_c. It is useful to divide the pressure dependence of J_c up into its time-independent (intrinsic) and time-dependent (relaxation) components

$$d \ln J_c/dP = (d \ln J_c/dP)_{intr} + (d \ln J_c/dP)_{relax}. \quad (4)$$

The relaxation fraction η is then defined by $\eta \equiv (d \ln J_c/dP)_{relax} - (d \ln J_c/dP)$ so that

$$(d \ln J_c/dP)_{intr} = (d \ln J_c/dP)(1 - \eta). \quad (5)$$

We first consider the relaxation contribution in more detail.

A. Relaxation contribution to pressure dependence of J_c

As discussed in the Introduction, it is well known that pressure-induced oxygen ordering effects in the high-T_c ox-

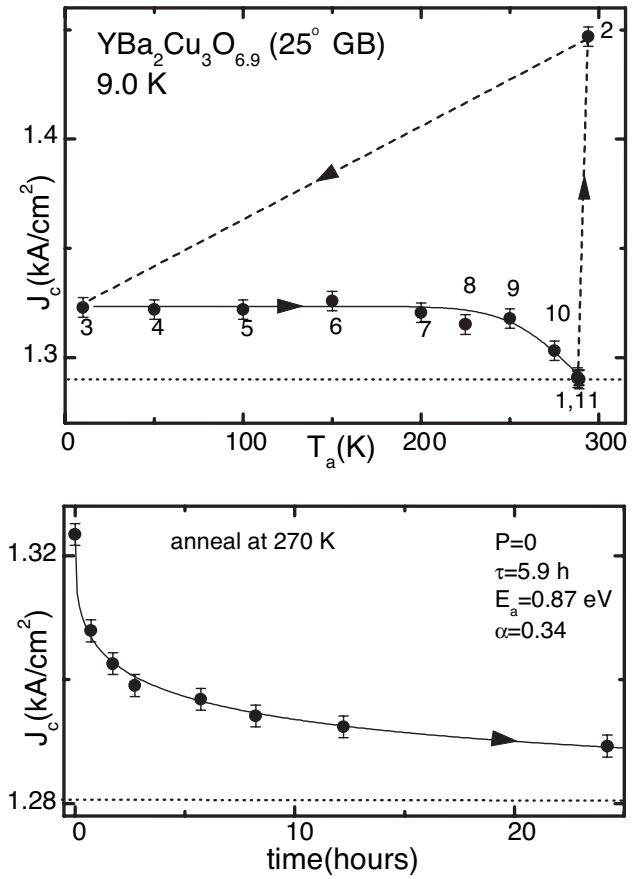

FIG. 18. For nearly optimally doped YBCO bicrystalline ring *d* with 25° GB: (upper) dependence of critical current density J_c at 9 K on annealing temperature T_a. Numbers give order of measurement. Solid line through data is guide to the eye. Horizontal dotted line marks initial value of J_c(9 K) at point 1. (lower) Dependence of J_c on time for fixed annealing temperature T_a=270 K following release of pressure at temperatures less than 50 K. Solid line is fit to data using Eq. (3). Horizontal dotted line in both graphs marks initial value of J_c(9 K) at point 1. Figure taken from Ref. 23.

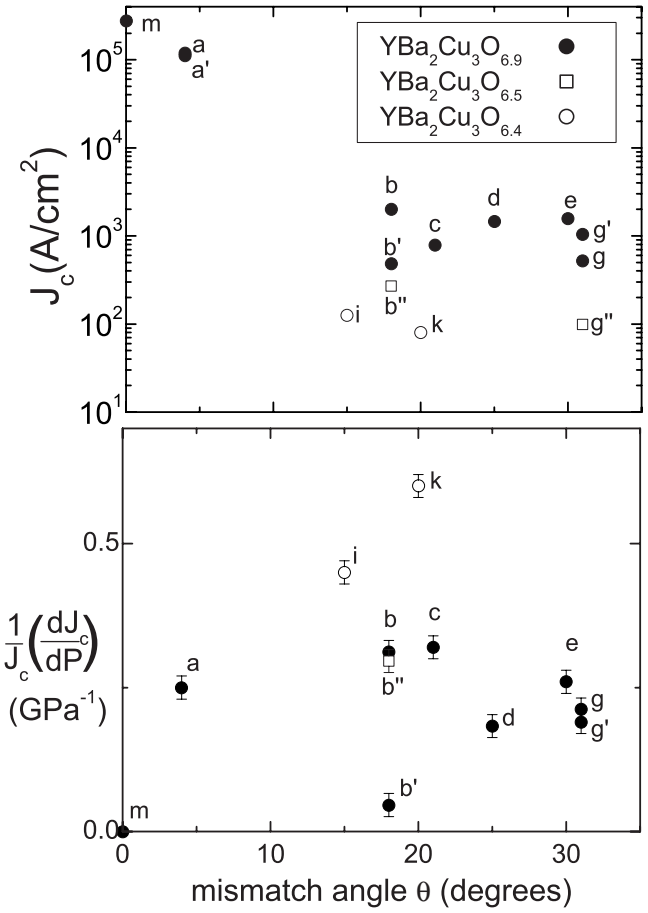

FIG. 19. Dependence of J_c at 9 K and its relative pressure derivative $J_c^{-1}(dJ_c/dP)$ on mismatch angle θ for all YBCO rings studied in the present experiments. Each lower-case letter (with or without primes) labels a ring with a specific GB mismatch angle θ: *m* −0°, *a*−4°, *i*−15°, *b*−18°, *k*−20°, *c*−21°, *d*−25°, *e*−30°, *g*−31°; the same labels are used in the text and Table I.

ides can have an important or even dominant influence on the pressure dependence of bulk properties, such as the value of T_c.[12–16] These relaxation effects are most significant when there are large numbers of mobile oxygen anions in a lattice containing a significant number of vacant oxygen sites. Oxygen-ordering effects would thus be anticipated in the critical current density J_c in YBCO and other copper-oxide superconductors if the GBs are oxygen deficient.[23] The mechanism for the positive value of $(d \ln J_c/dP)_{\text{relax}}$ is likely the same as for the positive or negative values of $(d \ln T_c/dP)_{\text{relax}}$ in the bulk, namely, that the application of pressure enhances the degree of local order in the oxygen sublattice which then leads to cation valence changes promoting the introduction of additional charge carriers into the GB region (for J_c) or the CuO_2 planes (for T_c). In fact, there are, to our knowledge, only three special cases where no pressure-induced oxygen ordering effects in bulk or GB properties would occur: (1) no mobile oxygen anions are present in the oxygen sublattice, (2) the oxygen sublattice is completely filled up with oxygen anions so that no change in the occupation of oxygen sites is possible, or (3) the property being measured is at an extremum versus oxygen concentration so that the property is unaffected by small changes in carrier concentration due to oxygen ordering.

The third case is illustrated in Fig. 8 for YBCO, where $T_c(x)$ passes through a maximum at $x \simeq 6.95$. At this oxygen concentration *no* relaxation effects in T_c are observed,[14] even though some oxygen-ordering effects certainly occur due to the presence of a 5% vacancy concentration in the CuO chains. In Fig. 8 it is also seen that across the same range of oxygen concentration x the critical current density $J_c(x)$ across the GB increases monotonically. Although the relative number of occupied oxygen sites in the GB region is almost certainly different from that in the bulk, as the oxygen concentration x in the bulk is increased, more vacant sites in the GB region are likely filled, leading to an increase in the carrier concentration in the GB and thus to an enhancement in J_c. We conclude that if relaxation effects are observed in J_c, this very fact implies that the oxygen sites in the GB region are only partially filled, i.e., empty oxygen sites are available. We thus propose that the presence or absence of relaxation effects in J_c is a useful diagnostic tool to test

whether or not the GB region is able to accommodate further oxygen anions and thus enhance J_c. This procedure also applies to materials containing an extremely large number of GBs, i.e., polycrystalline material, where ac susceptibility measurements can be separated into intragrain and intergrain contributions to determine J_c as a function of temperature and pressure.[20]

From the data in Figs. 16–18 above we concluded that the relaxation contribution to the strong enhancement of J_c under pressure amounted to $\eta \simeq 0.20$ for the nearly optimally doped ring d and to $\eta \simeq 0.65$ for the strongly underdoped ring k. From Table I we see that a sizeable relaxation contribution varying from 0.12 to 0.65 is present for all five rings where relaxation effects were studied. From this we conclude that YBCO bicrystalline rings, be they underdoped or nearly optimally doped, normally have vacant oxygen sites in the GB region. To fill all sites it may be necessary to expose the sample to simultaneous high-temperature and high-pressure oxygen treatments and then to seal the surface of the sample shut with a coating to prevent oxygen anions from escaping under ambient temperature/pressure conditions.

As seen in Table I, for four of the five rings studied, the intrinsic pressure derivative in Eq. (4), $(d \ln J_c/dP)_{\text{intr}}$, makes the dominant contribution to the total pressure derivative $d \ln J_c/dP$; only for the strongly underdoped ring k is the relaxation derivative larger. For example, for ring d in Fig. 18, as discussed above, the relaxation contribution according to Eq. (5) is $(d \ln J_c/dP)_{\text{intr}} = (d \ln J_c/dP)(1-\eta) \simeq 0.20(1-0.2) = 0.16\ \text{GPa}^{-1}$. A similar analysis for the underdoped ring k gives $(d \ln J_c/dP)_{\text{intr}} \simeq 0.59(1-0.65) = +0.21\ \text{GPa}^{-1}$. For all five samples studied (see Table I) the intrinsic contribution does not vary appreciably. Below we discuss possible origins for this intrinsic contribution.

It is interesting to note from Fig. 19 that the total pressure derivatives $(d \ln J_c/dP)$ for the underdoped samples studied (i and k) are somewhat larger than those for the optimally doped samples. Our results indicate that this enhancement may be due to the relatively large relaxation derivative $(d \ln J_c/dP)_{\text{relax}}$ for the underdoped samples.

B. Intrinsic contribution to pressure dependence of J_c

From the previous subsection we have learned that both intrinsic and relaxation effects make important contributions to the sizeable pressure dependence of J_c observed in the present experiments on YBCO bicrystals, intrinsic effects being larger for nearly optimally doped samples, whereas relaxation effects dominate for strongly underdoped bicrystals. For both doping levels, however, the intrinsic contribution remains relatively constant $(d \ln J_c/dP)_{\text{intr}} \simeq +0.14$ to $+0.25\ \text{GPa}^{-1}$. We would now like to discuss possible origins for this intrinsic contribution.

The actual mechanism by which a GB limits J_c in the high-T_c oxides is still a matter of controversy and will likely remain so until the mechanism for the superconducting pairing interaction itself has been identified. In their review, Hilgenkamp and Mannhart[3] have grouped the many possible GB mechanisms into five families: mechanisms based on (1) structural properties, (2) deviations from ideal stoichiometry, (3) order-parameter symmetry, (4) interface charging and band bending, and (5) direct suppression of the pairing mechanism. Rather than attempting to consider each of these possible scenarios individually, we consider for contreteness a particularly simple model whereby a GB is represented by a tunnel barrier with width W and height ϕ through which superconducting electron pairs can quantum mechanically tunnel, as illustrated in Fig. 20.[39,40] In the WKB approximation the current density through such a potential barrier is given by the expression

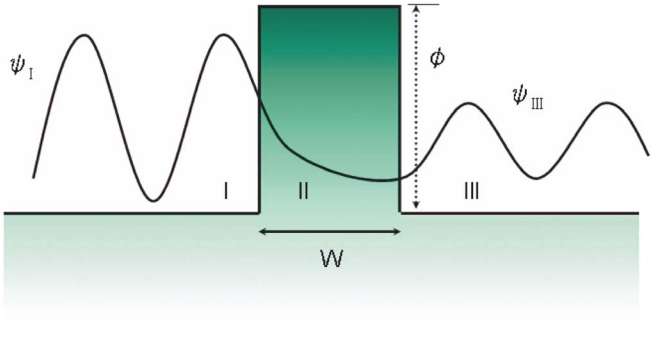

FIG. 20. (Color online) Schematic representation of the quantum mechanical tunneling of a wave ψ through a potential barrier with height ϕ and width W.

$$J_c = J_{c_0} \exp(-2KW), \tag{6}$$

where J_{c_0} is the critical current density for zero barrier width, i.e., no grain boundary, $K \equiv \sqrt{2m\phi}/\hbar$ is the decay constant, and ϕ is the barrier height. As seen in Fig. 14 and Table I for the nearly optimally doped YBCO ring m with no GB $J_c(0\ \text{K}) = J_{c_0} \simeq 275\,000\ \text{A cm}^{-2}$; within experimental error, however, we find $d \ln J_{c_0}/dP \approx 0$, as discussed above. From Eq. (6), therefore, we obtain for the relative pressure dependence of J_c

$$\frac{d \ln J_c}{dP} \simeq -\left[\left(\frac{d \ln W}{dP}\right)\ln\left(\frac{J_{c_0}}{J_c}\right)\right] - \frac{1}{2}\left[\left(\frac{d \ln \phi}{dP}\right)\ln\left(\frac{J_{c_0}}{J_c}\right)\right]. \tag{7}$$

The first term on the right makes a positive contribution to $d \ln J_c/dP$ since the barrier width W decreases under pressure. Assuming, as above, that $-d \ln W/dP \equiv \kappa_{\text{GB}} \approx \kappa_a \approx 2 \times 10^{-3}\ \text{GPa}^{-1}$,[37] we obtain for the $\theta = 25°$ ring in Fig. 6, where $J_c \simeq 1{,}450\ \text{A/cm}^2$ at low temperatures, the estimate $(-d \ln W/dP)\ln(J_{c_0}/J_c) \approx +0.01\ \text{GPa}^{-1}$, a value $20\times$ less than that from experiment $d \ln J_c/dP \simeq +0.20\ \text{GPa}^{-1}$. Within the simple tunneling barrier model, therefore, the strong enhancement in J_c under pressure does *not* arise from the compression of the GB width W alone, but requires a reduction in the barrier height ϕ at the GB. From Eq. (7) a pressure derivative of only $d \ln \phi/dP \simeq -0.072\ \text{GPa}^{-1}$ (a 7.2% decrease in ϕ per GPa pressure) would be sufficient to yield the experimental value $d \ln J_c/dP \simeq +0.20\ \text{GPa}^{-1}$.

We now carry out an identical calculation for the nearly optimally doped bicrystal a' with 4° GB where at low temperatures $J_c \simeq 112{,}000\ \text{A/cm}^2$, yielding $(-d \ln W/$

$dP)\ln(J_{c_0}/J_c) \approx +0.0018$ GPa^{-1}, a value 140× less than the experimental value $d \ln J_c/dP \simeq +0.25$ GPa^{-1} from Table I. This experimental value can be accounted for by the strong reduction in barrier height $d \ln \phi/dP \simeq -0.55$ GPa^{-1}. The same calculation for the 31° GB bicrystal *g*, where $J_c \simeq 520$ A/cm^2, yields $(-d \ln W/dP)\ln(J_{c_0}/J_c) \approx +0.017$ GPa^{-1}, a value 12× less than the experimental value $d \ln J_c/dP \simeq +0.21$ GPa^{-1} from Table I. This experimental value can be accounted for by the reduction in the barrier height $d \ln \phi/dP \simeq -0.062$ GPa^{-1}.

Similar results are obtained for the remaining nearly optimally doped samples. Since it is unlikely in YBCO that the compressibility of the GB is one or two orders of magnitude larger than the in-plane compressibility,[37] it is clear that the reduction in the barrier width under pressure is much too small to account for the sizeable intrinsic increase in the carrier density J_c under pressure. Within the tunnel barrier model, therefore, a reduction in the barrier height ϕ in the range $d \ln \phi/dP \simeq -0.05$ to -0.55 GPa^{-1} is necessary to account for the experimental results.

The barrier height ϕ in the tunnel-barrier model may be considered to represent important GB features in other models, such as the degree of lattice disorder, the carrier concentration, changes in the localized states, the degree of band bending, or changes in the pairing interaction. In view of the importance of oxygen ordering (relaxation) effects both in the bulk and GB, which appear to operate via changes in the carrier concentration *n*, it would seem likely that the large intrinsic increase in J_c under pressure is at least in part due to an enhancement in *n*. Indeed, in all high-T_c oxides, such as YBCO, which contain charge-reservoir layers, *n* in the bulk is invariably found to increase under pressure.[15,16,41] In most GB models, an increase in the carrier concentration strengthens the GB by, for example, reducing the GB potential through a shortened screening length, enhancing the pairing interaction, or reducing the effects of band bending.[3] Browning *et al.*[39] utilize a tunneling model where the effective barrier width W_{eff} is identified with the thickness of the nonsuperconducting zone at the grain boundary. Since W_{eff} increases linearly with the mismatch angle θ, the exponential dependence of J_c on θ for $\theta \geqslant 10°$ receives a natural explanation through Eq. (6). In this scenario a pressure-induced increase in the carrier concentration n_{GB} in the GB would significantly reduce the effective GB width W_{eff}, thus enhancing J_c.

In summary, the critical current density J_c across [001]-tilt GBs with mismatch angles in the range 4° to 31° in nearly optimally doped and strongly underdoped YBCO bicrystals is found to increase strongly with hydrostatic pressure, in most cases at a rate from +0.20 to +0.50 GPa^{-1}. This suggests a new procedure to enhance J_c at ambient pressure: compress the GB as much as possible through epitaxial growth or other chemical means. Within a simple tunnel barrier model, the rate of increase of J_c is far too large to be caused by the decrease in width *W* of a tunnel barrier alone; a moderate to strong decrease in the barrier height ϕ under pressure is indicated.

Sizeable pressure-induced oxygen ordering effects are found to occur in the GB, revealing that the value of J_c is a complicated function of the pressure/temperature history of the sample, i.e., $J_c = J_c(T,P,t)$, in analogy with the well studied relaxation processes in the bulk for the superconducting transition temperature $T_c = T_c(T,P,t)$.[12,13,16] These J_c relaxation effects are responsible for approximately 20% of the total increase in J_c with pressure in nearly optimally doped YBCO bicrystals, but increases to over 60% in strongly underdoped samples. The fact that these relaxation effects in J_c occur at all indicates that a significant concentration of vacant oxygen sites are present in the GB. Filling these vacant sites with oxygen anions, either by annealing the sample under high oxygen pressure at high temperature or through electro-chemical oxidation, will significantly increase the carrier concentration in the GB region and thus lead to further enhancements in J_c.

ACKNOWLEDGMENTS

The authors would like to thank M. Debessai for experimental assistance. The research at Washington University is supported by NSF Grant No. DMR-0404505 and that at the Argonne National Laboratory by the U.S. Department of Energy, Basic Energy Sciences-Materials Sciences, under Contract No. W-31-109-ENG-38.

[1] A. Schilling, M. Cantoni, J. D. Guo, and H. R. Ott, Nature (London) **363**, 56 (1993).

[2] For a brief expose of grain boundary properties, see J. Mannhart and P. Chaudhari, Phys. Today **54**, 48 (2001).

[3] For an excellent comprehensive review of grain boundaries in the cuprate oxides, see H. Hilgenkamp and J. Mannhart, Rev. Mod. Phys. **74**, 485 (2002).

[4] P. Chaudhari, J. Mannhart, D. Dimos, C. C. Tsuei, J. Chi, M. M. Oprysko, and M. Scheuermann, Phys. Rev. Lett. **60**, 1653 (1988).

[5] D. Dimos, P. Chaudhari, J. Mannhart, and F. K. LeGoues, Phys. Rev. Lett. **61**, 219 (1988).

[6] A. Schmehl, B. Goetz, R. R. Schulz, C. W. Schneider, H. Bielefeldt, H. Hilgenkamp, and J. Mannhart, Europhys. Lett. **47**, 110 (1999).

[7] G. Hammerl, A. Schmehl, R. R. Schulz, B. Goetz, H. Bielefeldt, C. W. Schneider, H. Hilgenkamp, and J. Mannhart, Nature (London) **407**, 162 (2000).

[8] X. Song, G. Daniels, D. M. Feldmann, A. Gurevich, and D. Larbalestier, Nature (London) **4**, 470 (2005).

[9] R. F. Klie, J. P. Buban, M. Varela, A. Franceschetti, C. Jooss, Y. Zhu, N. D. Browning, S. T. Pantelides, and S. J. Pennycook, Nature (London) **435**, 475 (2005).

[10] J. D. Jorgensen, B. W. Veal, A. P. Paulikas, L. J. Nowicki, G. W. Crabtree, H. Claus, and W. K. Kwok, Phys. Rev. B **41**, 1863 (1990).

[11] B. W. Veal, A. P. Paulikas, H. You, H. Shi, Y. Fang, and J. W. Downey, Phys. Rev. B **42**, 6305 (1990).
[12] A.-K. Klehe, C. Looney, J. S. Schilling, H. Takahashi, N. Môri, Y. Shimakawa, Y. Kubo, T. Manako, S. Doyle, and A. M. Hermann, Physica C **257**, 105 (1996).
[13] S. Sadewasser, J. S. Schilling, A. P. Paulikas, and B. W. Veal, Phys. Rev. B **61**, 741 (2000).
[14] W. H. Fietz, R. Quenzel, H. A. Ludwig, K. Grube, S. I. Schlachter, F. W. Hornung, T. Wolf, A. Erb, M. Kläser, and G. Müller-Vogt, Physica C **270**, 258 (1996).
[15] J. S. Schilling and S. Klotz, in *Physical Properties of High Temperature Superconductors*, edited by D. M. Ginsberg (World Scientific, Singapore, 1992), Vol. III, p. 59.
[16] B. Lorenz and C. W. Chu, in *Frontiers in Superconducting Materials*, edited by A. Narlikar (Springer Verlag, Berlin, 2005), p. 459.
[17] M. K. Wu, J. R. Ashburn, C. J. Torng, P. H. Hor, R. L. Meng, L. Gao, Z. J. Huang, Y. Q. Wang, and C. W. Chu, Phys. Rev. Lett. **58**, 908 (1987).
[18] D. Larbalestier, A. Gurevich, D. M. Feldmann, and A. Polyanskii, Nature (London) **414**, 368 (2001).
[19] M. R. Presland, J. L. Tallon, R. G. Buckley, R. S. Liu, and N. E. Flower, Physica C **176**, 95 (1991); J. L. Tallon, C. Bernhard, H. Shaked, R. L. Hitterman, and J. D. Jorgensen, Phys. Rev. B **51**, 12911 (1995).
[20] J. Diederichs, W. Reith, B. Sundqvist, J. Niska, K. A. Easterling, and J. S. Schilling, Semicond. Sci. Technol. **4**, S97 (1991).
[21] S. L. Bud'ko, M. F. Davis, J. C. Wolfe, C. W. Chu, and P. H. Hor, Phys. Rev. B **47**, 2835 (1993).
[22] H. Claus, U. Welp, H. Zheng, L. Chen, A. P. Paulikas, B. W. Veal, K. E. Gray, and G. W. Crabtree, Phys. Rev. B **64**, 144507 (2001).
[23] T. Tomita, J. S. Schilling, L. Chen, B. W. Veal, and H. Claus, Phys. Rev. Lett. **96**, 077001 (2006).
[24] J. D. Jorgensen, B. W. Veal, A. P. Paulikas, L. J. Nowicki, G. W. Crabtree, H. Claus, and W. K. Kwok, Phys. Rev. B **41**, 1863 (1990).
[25] J. E. Schirber, Cryogenics **10**, 418 (1970).
[26] H. Zheng, H. Claus, L. Chen, A. P. Paulikas, B. W. Veal, B. Olsson, A. Koshelev, J. Hull, and G. W. Crabtree, Physica C **350**, 17 (2001).
[27] Y. V. Sushko, B. DeHarak, G. Cao, G. Shaw, D. K. Powell, and J. W. Brill, Solid State Commun. **130**, 341 (2004).
[28] Th. Herzog, H. A. Radovan, P. Ziemann, and E. H. Brandt, Phys. Rev. B **56**, 2871 (1997).
[29] J. Jung, I. Isaac, and M. A.-K. Mohamed, Phys. Rev. B **48**, 7526 (1993).
[30] B. W. Veal, H. Claus, L. Chen, and A. P. Paulikas, Ceram. Trans. **140**, 309 (2003).
[31] V. R. Todt, X. F. Zhang, D. J. Miller, M. St. Louis-Weber, and V. P. David, Appl. Phys. Lett. **69**, 3746 (1996); K. E. Gray, M. B. Field, and D. J. Miller, Phys. Rev. B **58**, 9543 (1998).
[32] H. Claus, K. K. Uprety, B. Ma, A. P. Paulikas, V. K. Vlasko-Vlasov, U. Welp, B. W. Veal, and K. E. Gray, Physica C **416**, 1 (2004).
[33] H. Claus, B. Ma, A. P. Paulikas, Y. Tang, R. Nikolova, B. W. Veal, and K. E. Gray, *Proceedings of the 6th European Conference on Applied Superconductivity*, Sorrento, Italy, September 14–18, 2003, edited by A. Andreone, G. P. Pepe, R. Cristiano, and G. Masullo, *Institute of Physics Conference Series No. 181* (Institute of Physics, Bristol, 2004), p. 89.
[34] J. D. Jorgensen, S. Pei, P. Lightfoot, D. G. Hinks, B. W. Veal, B. Dabrowski, A. P. Paulikas, R. Kleb, and I. D. Brown, Physica C **171**, 93 (1990).
[35] C. P. Poole, Jr., H. A. Farach, and R. J. Creswick, in *Superconductivity* (Academic Press, New York, 1996), p. 51.
[36] J. P. Hirth and J. Lothe, *Theory of Dislocations* (McGraw-Hill, New York, 1968).
[37] In view of the fact that GBs contain vacancies and other structural defects, κ_{GB} is likely somewhat greater than κ_a. In YBCO, for example, the average linear compressibility in the CuO_2 plane increases by 17% if the oxygen concentration in the chains is reduced by 35% (see Ref. 34).
[38] F. C. Frank and J. H. van der Merwe, Proc. R. Soc. London, Ser. A **189**, 205 (1949); G. A. Prinz, MRS Bull. **XIII**, 28 (1988).
[39] N. D. Browning, J. P. Buban, P. D. Nellist, D. P. Norton, M. F. Chisholm, and S. J. Pennycook, Physica C **294**, 183 (1998); J. Halbritter, Phys. Rev. B **46**, 14861 (1992).
[40] J. Halbritter, Phys. Rev. B **46**, 14861 (1992).
[41] H. Takahashi and N. Môri, in *Studies of High Temperature Superconductors*, edited by A. V. Narlikar (Nova Science, New York, 1995), Vol. 16/17, p. 1.